Solid State Ionics 284 (2016) 7–13

Contents lists available at ScienceDirect

Solid State Ionics

journal homepage: www.elsevier.com/locate/ssi

Multifunctional ZrF_4 nanocoating for improving lithium storage performances in layered $Li[Li_{0.2}Ni_{0.17}Co_{0.07}Mn_{0.56}]O_2$

Xiaoping Zhang [a], Yue Yang [b], Shuwei Sun [a], Qing Wu [a], Ning Wan [a], Du Pan [a], Ying Bai [a,*]

[a] *Key Laboratory of Photovoltaic Materials of Henan Province and School of Physics & Electronics, Henan University, Kaifeng 475004, PR China*
[b] *College of Electronic Science & Engineering, Jilin University, Changchun 130012, PR China*

ARTICLE INFO

Article history:
Received 4 November 2015
Accepted 6 November 2015
Available online 10 December 2015

Keywords:
Electrochemical performances
Lithium-rich
Nanocoating

ABSTRACT

Layered $Li[Li_{0.2}Ni_{0.17}Co_{0.07}Mn_{0.56}]O_2$ is successfully synthesized by a sol–gel method and is further coated with ZrF_4 (0.5, 1, 2 and 3 wt.%) through a simple wet chemical strategy. Physical characterizations indicate that the ZrF_4 nanocoating layers have little impact on cathode structure. Comparison of electrochemical performances demonstrates that 1 wt.% ZrF_4 modified electrode exhibits the highest reversible capacity (193 mAh g^{-1}) and best cycling performance (capacity retention of 89%) after 100 cycles at 0.1 C. Electrochemical impedance spectroscopy (EIS) analysis reveals that charge transfer resistance grows much slower after coating. Fourier transform infrared (FTIR) results further confirm that the surface ZrF_4 effectively suppresses the fast growth of solid electrolyte interface (SEI) film. The improved electrochemical properties are thus attributed to the multifunctional ZrF_4 nanocoating layer, which not only suppresses the side reaction(s) and oxygen loss, but also accelerates the lithium ion transportation due to the reduced resistance. Additionally, differential scanning calorimetry (DSC) tests show that the ZrF_4 layer also helps in enhancing the thermal stability. This work provides a new insight into surface modification in achieving high energy cathodes for the next-generation lithium-ion batteries.

1. Introduction

Li-rich manganese-based layer-structured cathodes, which could be recognized as either $Li(Li_{1-x-y}Mn_xM_y)O_2$ or $xLi_2MnO_3{\cdot}(1-x)LiMO_2$ (M refers to commonly used transition metals such as Ni and Co), have attracted extensive interest in recent years [1,2]. The unique feature of these materials is their high reversible capacity (~300 mAh g^{-1}), which is nearly twice as high as those of $LiCoO_2$ and $LiFePO_4$ cathodes presently used in commercial lithium-ion batteries (LIBs) [3–5].

However, some key issues need to be addressed for this family of materials before their wide application: distinct voltage fade and poor cycling performance. Mitigating voltage drop and capacity decrease will enable the usage of these high-energy materials in plug-in hybrid electric vehicles (HEVs) and electric vehicles (EVs). The main origin of this deterioration during cycling is that the organic electrolytes are unstable, which tend to be decomposed on the surface of electrode at high voltages (>4.5 V) [6]. Additionally, there is a gradual transition from a layered structure to a spinel one. The cycling performance is therefore not so satisfactory for commercial applications.

Surface modification is an effective strategy to improve the electrochemical performances of cathodes by means of providing a protection layer to minimize the direct contact of active material with electrolyte and/or modifying surface chemistry [7]. Optimizing the surface region of layered oxide grains is of particular importance since the surface not only experiences Li insertion/extraction, but also serves as the interface between cathode and electrolyte. In this regard, various metal oxides are commonly used as coating materials [8–12]. Cho et al. [13] investigated a zero-strain $LiCoO_2$ cathode material produced by thin-film coating of high-fracture-toughness ZrO_2, which suppressed the phase transition during cycling and contributed to the best electrochemical performances compared with the other metal oxides. Later, another research confirmed that the ZrO_2 coating layer outside active material will be converted into ZrF_4 film during electrochemical cycling, which was more stable and effective against HF attack [14].

Herein, ZrF_4 is firstly applied to directly coat on the surface of $Li[Li_{0.2}Ni_{0.17}Co_{0.07}Mn_{0.56}]O_2$ cathode by a simple precipitation reaction. After the structures of the pristine and coated materials have been identified, the effects of ZrF_4 nanocoating on the electrochemical performance and thermal stability of the Li-rich cathode are systematically investigated. Obviously, compared with the pristine material, appropriated content of ZrF_4-coated sample shows significant improvements in initial columbic efficiency, rate capability and capacity retention. As another feature of this work, the improvement mechanism is also intensively explored.

---

* Corresponding author.
E-mail address: ybai@henu.edu.cn (Y. Bai).

http://dx.doi.org/10.1016/j.ssi.2015.11.028

2. Experimental

Bare Li[$Li_{0.2}Ni_{0.17}Co_{0.07}Mn_{0.56}$]$O_2$ was synthesized by a sol–gel method. Stoichiometric amounts of $CH_3COOLi{\cdot}2H_2O$, $Ni(CH_3COO)_2{\cdot}4H_2O$, $Co(CH_3COO)_2{\cdot}4H_2O$ and $Mn(CH_3COO)_2{\cdot}4H_2O$ were dissolved in ethyl alcohol respectively. Then the solutions were dropwise added into a citric acid solution with vigorous stirring. The obtained solution was evaporated at 80 °C with continuous stirring until a transparent sol was formed, which was afterwards put into a drying oven for 12 h to obtain the corresponding gel. Next, the gel was transferred into a chamber furnace and preheated at 450 °C for 10 h. Finally, the gathered powder was ground and calcined at 900 °C in air for 12 h to obtain the target material.

To prepare ZrF_4-coated Li[$Li_{0.2}Ni_{0.17}Co_{0.07}Mn_{0.56}$]$O_2$, $Zr(NO_3)_4{\cdot}5H_2O$ and NH_4F were separately dissolved in distilled water. Afterwards, the as-prepared Li[$Li_{0.2}Ni_{0.17}Co_{0.07}Mn_{0.56}$]$O_2$ powder was homogeneously dispersed in $Zr(NO_3)_4{\cdot}5H_2O$ solution. Then, the NH_4F solution was added slowly with vigorous stirring. After the reaction was completed, the mixture was filtered and washed repeatedly with distilled water before drying at 100 °C for 10 h. The molar ratio of Zr to F was adjusted to be 1:4. There is possibly a little discrepancy in the exact molar ratio between Zr and F in the surface coating layer since the accurate content of F is very difficult to be measured. Nevertheless, for simplicity, the obtained Zr—F compound modified Li[$Li_{0.2}Ni_{0.17}Co_{0.07}Mn_{0.56}$]$O_2$ was named as ZrF_4-coated Li[$Li_{0.2}Ni_{0.17}Co_{0.07}Mn_{0.56}$]$O_2$ based on its nominal ratio hereafter. The amounts of ZrF_4 were set at 0.5, 1, 2 and 3 wt.%. Finally, the dried powders were collected and calcined at 400 °C for 5 h to obtain the target materials.

X-ray diffraction (XRD) patterns of the samples were measured on Bruker D8 Advance diffractometer (Bruker, Germany) with the slit size of 0.6 mm and Cu Kα radiation of $\lambda \sim 0.15418$ nm between 10° and 80° at a scan rate of 0.04° s^{-1}. The Raman spectra were collected on a laser Raman Spectrometer (RM-1000, Renishaw) with 633 nm He—Ne laser. Fourier transform infrared (FTIR) measurements were performed on Nicolet AVATAR360 Fourier-transformed infrared spectrometer. For postmortem FTIR and XRD measurements, the cycled cells were carefully disassembled in glovebox and the extracted electrodes were afterwards repeatedly rinsed by dimethyl carbonate (DMC). Then the cycled electrodes were evacuated thoroughly in a transition chamber before measurement. The surface morphologies were observed through field emission scanning electron microscopy (FESEM, JEOL 7001F). Electron diffraction spectroscopy (EDS) was applied to determine the element composition together with FESEM in a large field of view. The images of high resolution transmission electron microscopy (HRTEM) were collected on FEI Tecnai F20 equipment to investigate the microstructure of samples. The inductively coupled plasma (ICP) analysis was performed on Thermo Fisher ICAP 6300 to determine the exact chemical compositions of the samples. Differential scanning calorimetry (DSC) analysis was carried out on TA Q600 by sealing the charged cathode (4.8 V at galvanostatic 0.1 C) in an Al crucible in dry Ar and heated from room temperature to 400 °C at a rate of 5 °C min^{-1}.

The obtained samples, acetylene black, and polyvinylidene fluoride, (PVDF, as binder) were mixed at a weight ratio of 70:15:15, and compressed to prepare the working electrode. A metallic lithium foil was used as the counter electrode. The half cell was composed of a cathode and a lithium metal anode, separated by a Celgard 2400 porous polypropylene film as separator. The electrolyte was $LiPF_6$ (1 M) in a mixture of ethylene carbonate (EC) and DMC with a volume ratio of 1:1. In the galvanostatic test, the assembled cells were cycled on a tester (Neware CT-2001A, China) between 2.0 and 4.8 V (vs. Li/Li^+) with a current density of 0.1 C (1 C = 378 mA g^{-1}) at room temperature. The electrochemical impedance spectroscopy (EIS) investigations were performed on an electrochemical workstation (CHI660C, Shanghai Chenhua) with three-electrode system over a frequency range from 100 kHz to 5 mHz in the charged state of 4.8 V after the cells were aged for two days to reach equilibrium.

3. Results and discussion

XRD patterns of Li[$Li_{0.2}Ni_{0.17}Co_{0.07}Mn_{0.56}$]$O_2$ before and after ZrF_4 surface modification are shown in Fig. 1. All the major diffraction peaks can be indexed to a layered oxide lattice based on a hexagonal α-$NaFeO_2$ type structure with a space group R$\overline{3}$m [15]. The clear splitting of (006)/(102) and (108)/(110) doublets indicates the as-prepared cathode material owns a well-organized layered structure [16–18]. The weak peaks between $2\theta = 20$–25° are reflected by a monoclinic unit cell with a C2/m symmetry, due to a $LiMn_6$ cation arrangement that occurs in the transition metal layers of Li_2MnO_3 region [19]. However, the intensity of the super-ordering peaks (020) and (110) obviously decreases after ZrF_4 coating, suggesting the reduction of Li_2MnO_3 phase. These results indicate that the ZrF_4-coated materials may contain some spinel oxides, which are converted from Li_2MnO_3. Nevertheless, no diffraction peak belonging to spinel phase could be clearly observed, which may be ascribed to its low content. Furthermore, there is no diffraction peak from ZrF_4 in the profiles, which may due to its amorphous phase calcined at a low temperature of 400 °C [20] and/or low content. Typically, no peak shift can be observed in partial enlarged view of (101), indicating that no big structure change in medical modification process. Comparatively, as can be seen from Fig. S1, after 1, 3 and 5 electrochemical cycles, the ZrF_4-coated materials exhibit reflections corresponding to the cubic spinel structure at 2θ° values of 44.1° (marked in asterisk). Interestingly, the diffraction peaks of the 1 wt.% ZrF_4-coated materials shifts gradually to a smaller angle when partial zoomed in (the (101) peaks are typically compared in the inset of Fig. S1). The clear peak shift implies that the original layered structure may have partially transformed into a new structure which is likely to be a spinel one [21].

Raman spectra are employed to detect the surface compositional and structural information of the as-prepared pristine and ZrF_4-coated Li-rich samples, which are presented in Fig. S2. For all the five curves, the vibrations centered at 590 cm^{-1} are comprised of bands at 554 cm^{-1} (Ni—O), 594 cm^{-1} (Mn—O) and 486 cm^{-1} (Co—O) [22]. FTIR spectra of the pristine and ZrF_4-coated Li-rich samples are exhibited in Fig. S3. The vibrations at 535 cm^{-1} and 615 cm^{-1} are apparent in all the four profiles, which could be ascribed to the asymmetric stretching of Li—O bonds [23] and the asymmetric stretching of Co—O bonds in CoO_6 octahedrons [24]. A weak band at 1634 cm^{-1} is assigned to the ambient O—H vibration [25,26]. Apparently, the results of Raman and FTIR show that the Li[$Li_{0.2}Ni_{0.17}Co_{0.07}Mn_{0.56}$]$O_2$ samples have similar surface conditions before/after ZrF_4 surface coating. The lack of vibration mode of spinel and ZrF_4 may be attributed to their low content.

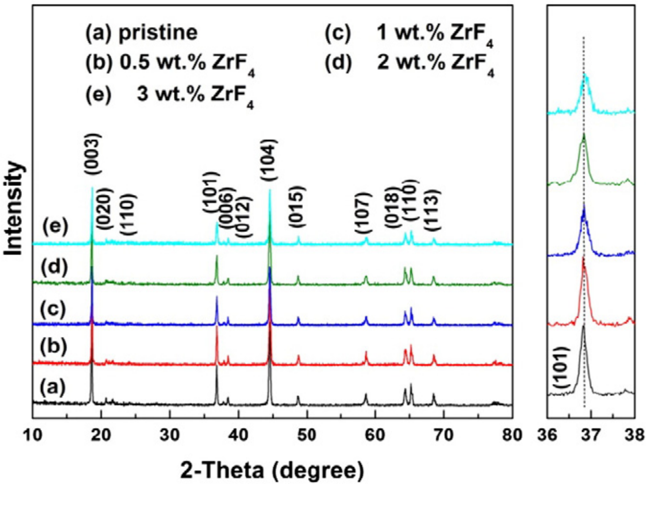

Fig. 1. XRD patterns of Li[$Li_{0.2}Ni_{0.17}Co_{0.07}Mn_{0.56}$]$O_2$ before and after ZrF_4 surface modification.